Colloid Polym Sci 276:893–902 (1998)
© Steinkopff Verlag 1998

ORIGINAL CONTRIBUTION

S.F. Lascelles
G.P. McCarthy
M.D. Butterworth
S.P. Armes

Effect of synthesis parameters on the particle size, composition and colloid stability of polypyrrole–silica nanocomposite particles

Received: 5 March 1998
Accepted: 27 April 1998

British Crown Copyright 1998/DERA.
Published with the permission of the controller of Her Brittannic Majesty's Stationery Office

S.F. Lascelles · G.P. McCarthy
M.D. Butterworth · S.P. Armes (✉)
School of Chemistry
Physics and Environmental Science
University of Sussex
Falmer, Brighton, BN1 9QJ
UK
E-mail: S.P. Armes@sussex.ac.uk

Abstract The effect of varying the oxidant, monomer and silica sol concentrations, silica sol diameter, polymerization temperature, stirring rate and oxidant type, on the particle size, polypyrrole content and conductivity of the resulting polypyrrole–silica colloidal nanocomposites has been studied. Surprisingly, nanocomposite formation appears to be relatively insensitive to most of the above synthesis parameters. One synthesis parameter which does have a significant and reproducible effect is the stirring rate: smaller, more monodisperse nanocomposite particles are obtained from rapidly stirred reaction solutions. However, this effect is only observed for the $(NH_4)_2S_2O_8$ oxidant. An alternative oxidant, H_2O_2/Fe^{3+}, was found to give nanocomposites of similar particle size, polypyrrole content and conductivity to those obtained using the $(NH_4)_2S_2O_8$ oxidant. The colloid stability of these polypyrrole–silica nanocomposite particles depends on their silica content. The colloid stability of a silica-rich nanocomposite prepared using the $(NH_4)_2S_2O_8$ oxidant in the presence of electrolyte was comparable to that of a silica sol, whereas a polypyrrole-rich nanocomposite prepared using $FeCl_3$ had markedly poorer colloid stability under these conditions. These observations are consistent with a charge stabilization mechanism for these nanocomposite particles.

Key words Conducting polymer – polypyrrole – silica – nanocomposite – synthesis

Introduction

Polypyrrole is a relatively air-stable organic conducting polymer. It is generally considered to be insoluble in all known solvents, probably due to some degree of cross-linking [1]. One approach to improving the processability of this otherwise intractable material is to synthesize polypyrrole in colloidal form. Usually, this has been achieved by aqueous dispersion polymerization using a suitable water-soluble polymer as a steric stabilizer [2–5].

Recently we have shown that polypyrrole colloids can be prepared in the absence of a polymeric stabilizer. In this approach, pyrrole is chemically polymerized in the presence of ultrafine silica [6, 7] or tin (IV) oxide [8, 9] sols. The precipitating conducting polymer coats the sol particles and "glues" them together. Under appropriate conditions colloidally stable polypyrrole–silica (or polypyrrole-tin(IV) oxide) "raspberry" particles can be obtained (see Fig. 1). Average particle diameters can be systematically varied from 100 to 300 nm and reasonably narrow size distributions were obtained in some cases. Polypyrrole loadings were up to 70% by mass, with pressed pellet conductivities as high as 4 $S\,cm^{-1}$ found for the polypyrrole–silica particles.

0 021

Colloid & Polymer Science, Vol. 276, No. 10 (1998)
© Steinkopff Verlag 1998

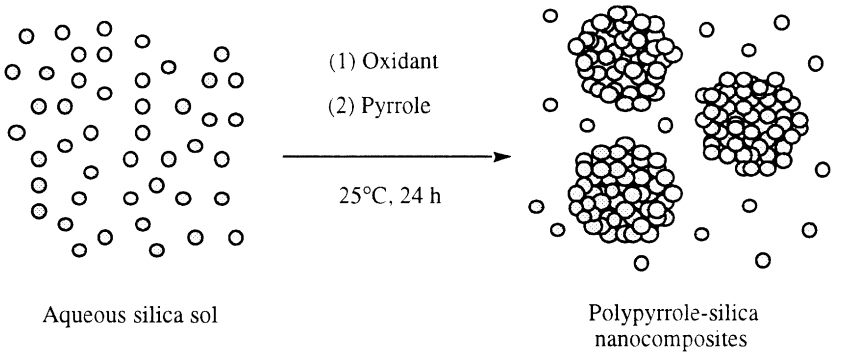

Fig. 1 Schematic representation of the formation of polypyrrole–silica nanocomposites

Zeta potential measurements indicated that the surfaces of the polypyrrole–silica "raspberry" particles were silica-rich, which accounts for their excellent long-term colloid stability [10]. Surface Si/N atomic ratios determined for these nanocomposites using X-ray photoelectron spectroscopy [11] were always significantly higher than the corresponding bulk Si/N ratios, which is consistent with the zeta potential data. BET surface area measurements [12] using nitrogen adsorbate at 77 K indicated that some of these nanocomposites particles have significant microporosity. Colloidal nanocomposites can also be formed with other conducting polymers such as polyaniline [13, 14] and poly(3,4 ethylenedioxythiophene) [15]. Small angle X-ray scattering studies [16] confirmed that the average separation distance between silica particles within polyaniline–silica raspberries is less than 5 nm. Thus, the conducting polymer component is dispersed within the raspberry particles at, or near, the molecular level and these composite materials can be regarded as true nanocomposites. It has been suggested that polypyrrole–silica dispersions have some potential as novel "marker" particles for immunodiagnostic assays [17, 18]. Here, the attractive feature of these novel particles is their intense intrinsic colouration, rather than their electrical conductivity. Ideally, such applications require surface-functionalized particles to aid the specific binding of the biological molecule of interest (e.g. proteins, antigens, antibodies, etc.). In this context we have recently demonstrated that carboxylic acid groups can be readily introduced during the nanocomposite synthesis simply by copolymerizing pyrrole with carboxylic acid-functionalized pyrrolic comonomers in the presence of an ultrafine silica sol. [19, 20].

In the present work we have investigated the effect of several synthesis parameters on the particle size, conducting polymer content and conductivity of the polypyrrole–silica nanocomposites. These include pyrrole, oxidant, and silica sol concentrations, silica sol diameter, polymerization temperature, oxidant type and stirring rate. In addition, the relative colloid stability of these nanocomposites in the presence of electrolyte has been assessed by turbidimetry.

Experimental

Chemicals and reagents

Pyrrole (BASF) was purified using a column of activated basic alumina and then stored at −15 °C in the absence of light prior to use. $FeCl_3 \cdot 6H_2O$, $(NH_4)_2S_2O_8$, H_2O_2 (27.5 wt% aqueous solution), and HBr (48% aqueous solution) were obtained from Aldrich Chemicals Ltd, and were used without further purification. The ultrafine colloidal silica sols of 20 nm diameter (40 wt% solids in water) and 2 nm diameter (15 wt% solids in water) were kindly donated by Nyacol Products, USA. Colloidal silica sols of 50, 100 and 300 nm diameter (supplied at 40, 20 and 20 wt% solids in water, respectively) were provided courtesy of Nissan Chemical Industries Ltd., Japan. All reactions were carried out using deionized water.

Effect of temperature

Reactions at room temperature were carried out as follows: The oxidant (9.10 g $FeCl_3 \cdot 6H_2O$, or 3.12 g $(NH_4)_2S_2O_8$) was added to a 200 ml screw-cap bottle containing a magnetic stirrer bar. The silica sol was then added (2.50 g of a 40 wt% solution of a 20 nm diameter sol), followed by the addition of deionized water, up to a total solution volume of 100 ml. Pyrrole (1.00 ml) was then added via syringe to this stirred solution, and the polymerization was allowed to proceed for 24 h. The resulting reaction solution was centrifuged at 5000 rpm for 30 min, and the supernatant containing the excess silica sol and inorganic byproducts was decanted and discarded. The black sediment was then redispersed in deionized

water. This centrifugation–redispersion cycle was repeated three times in order to remove excess non-aggregated silica and soluble (in)organic by-products.

Polypyrrole bulk powders were synthesized as described above, but in the absence of any colloidal silica sol. After the specified reaction time, the precipitated polypyrrole powders were vacuum-filtered and washed with copious amounts of deionized water until the washings were clear.

In the reduced temperature experiments, the general procedure described for the room temperature experiments was followed, except that the oxidant/silica solution was cooled to 0 °C in an ice bath prior to the addition of the pyrrole monomer; this temperature was maintained for the duration of the reaction. Similarly, in the elevated temperature experiments, the oxidant/silica solution was heated to 50 °C in a water bath with continuous stirring prior to pyrrole addition. Again, this temperature was maintained for the duration of the reaction.

Effect of reagent concentration

(1) Variation of silica and pyrrole concentration. In this set of experiments the oxidant concentration was fixed (9.10 g $FeCl_3 \cdot 6H_2O$ in 100 ml water) but the pyrrole and silica concentrations were varied. Thus, for entry 13 the $FeCl_3$ was in excess, for entry 14 the oxidant: monomer molar ratio was the theoretical stoichiometry of 2.33:1 and for entries 15–17 the pyrrole was in excess. All polymerizations were carried out at room temperature for 24 h. The clean-up procedure for the resulting nanocomposites was as described in the previous section.
(2) Variation of silica, pyrrole and oxidant concentrations. In this set of experiments the pyrrole and silica concentrations were varied as described in the previous section, but this time the $FeCl_3 \cdot 6H_2O$ oxidant was also varied in order to maintain a constant oxidant: monomer molar ratio of 2.33:1 (i.e. 9.10 g $FeCl_3 \cdot 6H_2O$ for 1.00 ml of pyrrole, 18.15 g for 2.00 ml of pyrrole, etc.). In this set of experiments both the yields and the rates of reaction increased with increasing reagent concentrations. All polymerizations were carried out at room temperature for 24 h. Dispersions were cleaned up by repeated centrifugation–redispersion cycles in deionized water.

Effect of silica particle diameter

The effect of varying the silica sol diameter on the final particle size of the nanocomposites was investigated using silica sols with nominal manufacturers' diameters of 20, 50, 100 and 300 nm in conjunction with $FeCl_3 \cdot 6H_2O$ (9.10 g). Experiments using 20 and 50 nm diameter silica were carried out using 1.00 and 2.50 g dry weight of silica, respectively, and experiments using 100 and 300 nm diameter silica were carried out using 5.00 and 15.00 g dry weight of silica respectively. Thus the nominal total surface area of silica sol was held constant at approximately 140 m^2 in each experiment. Pyrrole (1.00 ml) was then added via syringe, and the reaction was allowed to proceed for 24 h. Once the reaction was complete, the dispersions were cleaned by repeated centrifugation and redispersion in deionized water, except in the case of the nanocomposite prepared using 300 nm diameter silica. In this case the polypyrrole–silica particles were sufficiently large and/or flocculated to be purified by gravitational sedimentation–redispersion cycles.

Syntheses using hydrogen peroxide oxidant

In these syntheses H_2O_2 (2.00 ml; 27.5% sol in water), HBr (1.00 ml; 48% sol in water) and a catalytic amount of $FeCl_3 \cdot 6H_2O$ (0.10 ml of a 0.10 M solution) were added in turn to a 100 ml screw-cap bottle containing a magnetic flea. The silica sol was then added (4.38 g of a solution of 40 wt% solids of 20 nm diameter silica particles), followed by the addition of deionized water, up to 40 ml. Pyrrole (1.00 ml) was then added via syringe, and the reaction was allowed to proceed for 24 h. The resulting particles were purified as described earlier.

Effect of stirring rate

$(NH_4)_2S_2O_8$ (19.2 g) was dissolved in deionized water (85 ml). Silica sol (51.0 g of a 34 wt% aqueous solution, i.e. 17.34 g dry weight silica; ex. Nyacol products) was added and this solution was made up to 500 ml with deionized water. This reaction mixture was stirred at 4 °C for 10 min at 3000 rpm using a Silverson Laboratory mixer (model L4R). The stirring rate was increased to 5000 rpm and then pyrrole (5.0 ml) was added via syringe. The reaction mixture immediately turned black and stirring was continued for 30 min prior to clean-up via three centrifugation/redispersion cycles.

Characterisation of the polypyrrole–silica nanocomposites

Chemical composition. After clean-up, polypyrrole–silica dispersions were oven-dried overnight at 60 °C prior to

© Steinkopff Verlag 1998

CHN elemental microanalyses at an independent laboratory (Medac Ltd at Brunel University, UK).

Particle size analysis. The polypyrrole–silica nanocomposites were sized using disc centrifuge photosedimentometry (DCP). All measurements were carried out using a Brookhaven BI-DCP instrument, operating in the line start mode. Samples for DCP analysis were prepared by adding a few drops of the aqueous nanocomposite dispersion to 3 ml of a 1:2 v/v% methanol:water mixture. This solution was immersed in an ultrasonic bath for up to 10 min just prior to DCP analysis. The centrifuge rate was adjusted according to the size of the particles being measured. Typically, centrifugation rates were in the 1000 to 6000 rpm range. The densities of polypyrrole and silica were measured to be 1.46 and 2.17 g cm^{-3}, respectively, as measured by helium pycnometry. Assuming additivity, particle densities were calculated from the polypyrrole contents of the nanocomposites as determined from CHN microanalyses. In the DCP analyses it was assumed that the polypyrrole–silica nanocomposites had the same scattering characteristics as carbon black.

Conductivity measurements. The conductivities (σ) of compressed pellets of the dried nanocomposites were determined using the standard four-point probe method at room temperature. Random errors associated with these measurements are estimated to be $\pm 10\%$, with an additional systematic error of ca. 5–10%.

Colloid stability measurements. With the $FeCl_3 \cdot 6H_2O$-synthesized polypyrrole–silica particles, 2.75 g of a 40 wt% aqueous solution of 20 nm diameter silica (i.e. 1.10 g dry weight of silica) was used. With the $(NH_4)_2S_2O_8$-synthesized polypyrrole–silica particles, 8.50 g of a 40 wt% aqueous silica sol (i.e. 3.4 g dry weight of silica) of 20 nm diameter was used. Polymerizations were carried out at room temperature for 24 h, prior to clean-up via repeated centrifugation/redispersion cycles. The relative colloid stabilities of the above two polypyrrole–silica dispersions and also a silica sol of ca. 100 nm were assessed at 25 °C in the presence of 0.10 M KCl. Absorbance vs. time measurements were carried out using a Perkin Elmer Lambda 2S UV-vis spectrophotometer operating at a fixed wavelength of 500 nm. A second series of absorbance vs. time measurements were also made on the $(NH_4)_2S_2O_8$-synthesized polypyrrole–silica particles at KCl concentrations of zero, 0.01, 0.10 and 1.00 M KCl. In both sets of experiments a decrease in the normalized absorbance ratio (A_t/A_0) represented a reduction in colloid stability.

Results and discussion

The original aim of this fundamental study was to vary several nanocomposite synthesis parameters systematically in order to control particle size, conducting polymer content and electrical conductivity. Reasonably good control over particle size (i.e. 500 mm to 20 μm) had already been reported by Iler and McQueston in the patent literature for the preparation of analogous polymer-silica nanocomposites [21]. In this earlier work the polymeric component of the nanocomposites was a urea-formaldehyde resin synthesized by step polymerization chemistry. The redox chemistry used to prepare polypyrrole in the present study is obviously quite different. Nevertheless, Maeda and Armes had previously reported that the particle size and chemical composition (silica content) of the polypyrrole–silica nanocomposites could be systematically adjusted over a useful range by varying just two parameters, the silica sol concentration and the nature of the oxidant [6, 7]. In particular it was anticipated that the particle size range of the nanocomposites could be extended by examining additional synthesis parameters. These are considered in turn below.

Effect of temperature

Precipitation polymerization. Polypyrrole bulk powders were synthesized as reference materials (see Table 1) to enable determination of the polypyrrole contents of the analogous polypyrrole–silica particles. Thus the nitrogen

Table 1 Effect of reaction temperature on the yield and conductivity of polypyrrole bulk powders synthesized in the absence of any silica sol

Sample ID	Reaction temp. [°C]	Oxidant type	Reaction time [h]	PPY yield [%]	σ[a)] [S cm^{-1}]
1	0	$FeCl_3 \cdot 6H_2O$	24	94	12
2	25	$FeCl_3 \cdot 6H_2O$	24	93	16
3	50	$FeCl_3 \cdot 6H_2O$	4	98	1
4	0	$(NH_4)_2S_2O_8$	18	86	0.6
5	25	$(NH_4)_2S_2O_8$	18	84	0.6
6	50	$(NH_4)_2S_2O_8$	1	50	0.2

Reactions were carried out in 100 ml water, using 1.00 ml pyrrole at an oxidant:pyrrole molar ratio of 2.33:1.
[a)] By four-point probe method on compressed pellets.

content of the nanocomposite was compared with that of the most appropriate bulk powder. The data presented in Table 1 indicates that the polymerization temperature has a surprisingly small effect on the conductivity of polypyrrole bulk powders in the 0–50 °C range. The conductivities of polypyrroles synthesized using the $FeCl_3$ oxidant are usually around an order of magnitude higher than those prepared using $(NH_4)_2S_2O_8$. Maeda and Armes [7] attributed these differences to over-oxidation of the polypyrrole chains by the latter oxidant; FTIR studies provided some evidence for this hypothesis. The slightly lower conductivities obtained at 50 °C with either oxidant in the present study are probably also due to over-oxidation of the polypyrrole backbone, leading to reduced conjugation of the polypyrrole chains.

Excellent polypyrrole yields were generally obtained. However, using the $(NH_4)_2S_2O_8$ oxidant at 50 °C results in a significantly lower yield of only 50% (see entry 6 in Table 1). It is very likely that this reduced yield is due to the well-known thermal decomposition of $(NH_4)_2S_2O_8$ into sulfate radical anions at this temperature. Although capable of polymerizing a wide range of vinyl monomers, the resulting radical anions cannot polymerize pyrrole, therefore loss of $(NH_4)_2S_2O_8$ via this side reaction would necessarily lead to lower polypyrrole yields.

Table 2 shows the effect of varying the reaction temperature and oxidant type on the polypyrrole contents, particle size and electrical conductivities of the resulting polypyrrole–silica nanocomposites. Entries 7–9 were synthesized using the $FeCl_3 \cdot 6H_2O$ oxidant, and entries 10–12 were synthesized using the $(NH_4)_2S_2O_8$ oxidant. For both oxidants, varying the polymerization temperature between 0 and 50 °C had surprisingly little effect on either the weight-average particle diameter or the particle size distribution (PSD). The same temperature range was recently investigated by Riede et al. [22] for the synthesis of polyaniline-silica nanocomposite particles. It is noteworthy that these workers reported that stable colloidal dispersions could not be obtained above 30 °C. As with the bulk powder syntheses, polymerizations at 0 °C led to nanocomposites with the highest conductivities. Slightly smaller particle diameters were also obtained under these conditions.

According to the data presented in Table 2, polypyrrole–silica particles synthesized using $FeCl_3 \cdot 6H_2O$ have significantly higher conductivities than those synthesized using $(NH_4)_2S_2O_8$. Generally, the former nanocomposites also have higher polypyrrole loadings and larger particle diameters. These results are in general agreement with previous work published by Maeda and Armes [7].

Effect of varying pyrrole and silica concentrations

The data in Table 3 reveals that the "standard" formulation for polypyrrole–silica syntheses (i.e. 1.00 ml pyrrole, 1.00 g dry weight of silica in 100 ml of reaction solution, entry 14) yields relatively monodisperse particles with a weight-average diameter of 240 ± 50 nm. A representative transmission electron micrograph of these particles is shown in Fig. 2. This nanocomposite also had a relatively high conductivity (ca. 1 S cm^{-1}). These results are in very good agreement with those of Maeda and Armes and therefore serve to demonstrate the excellent batch-to-batch reproducibility of these nanocomposite syntheses [7]. Increasing both the pyrrole and the silica concentrations at a fixed oxidant concentration produced apparently larger particles, but with significantly broader particle size distributions (entries 15–17). These nanocomposites have much lower electrical conductivities ($< 10^{-6}$ S cm^{-1}). These observations are particularly surprising given that the volume fractions of polypyrrole in these nanocomposites (0.66–0.73) are significantly higher than the threshold value of 0.16 expected on the basis of classical percolation theory.

Table 2 Effect of reaction temperature on the particle size, conductivity and chemical composition of the resulting polypyrrole–silica nanocomposites

Sample ID	Reaction temp [°C]	Oxidant type	Reaction time [h]	PPY content[a] [wt%]	σ[b] [S cm^{-1}]	Weight-average diameter[c] [nm]
7	50	$FeCl_3 \cdot 6H_2O$	4	62.6	0.2	270 ± 70
8	25	$FeCl_3 \cdot 6H_2O$	24	61.6	1	250 ± 50
9	0	$FeCl_3 \cdot 6H_2O$	24	52.5	3	220 ± 60
10	50	$(NH_4)_2S_2O_8$	1	49.7	8×10^{-3}	170 ± 40
11	25	$(NH_4)_2S_2O_8$	24	51.8	6×10^{-3}	180 ± 40
12	0	$(NH_4)_2S_2O_8$	18	52.2	0.5	150 ± 50

Reactions were carried out in 100 ml water, using 1.00 ml pyrrole, an oxidant : pyrrole molar ratio of 2.33 : 1 and 1 g dry weight of 20 nm diameter silica sol.
[a] By CHN elemental microanalysis.
[b] By four-point probe method on compressed pellets.
[c] By disc centrifuge photosedimentometry.

Colloid & Polymer Science, Vol. 276, No. 10 (1998)
© Steinkopff Verlag 1998

Table 3 Effect of varying the pyrrole and silica concentrations at a fixed $FeCl_3$ concentration (corresponding to that required to polymerise 1.00 ml pyrrole) on the particle size, conductivity and chemical composition of the resulting polypyrrole–silica nanocomposites

Sample ID	Pyrrole concn. [w/v%]	Silica concn. [w/v%]	PPY content[a] [wt%]	σ[b] [S cm^{-1}]	Weight average diameter[c] [nm]
13	0.50	0.50	81.1	2	280 ± 110
14	1.00	1.00	59.8	1	240 ± 50
15	2.00	2.00	64.5	$<10^{-6}$	330 ± 70
16	3.00	3.00	54.3	$<10^{-6}$	890 ± 220
17	4.00	4.00	57.1	$<10^{-6}$	1070 ± 400

The polymerizations were carried out at 25 °C for 24 h using a 20 nm diameter silica sol in 100 ml water.
[a] By CHN elemental microanalysis.
[b] By four-point probe method on compressed pellets.
[c] By disc centrifuge photosedimentometry.

Table 4 Effect of varying the pyrrole, silica and oxidant concentrations on the particle size, conductivity and chemical composition of the resulting polypyrrole–silica nanocomposites

Sample ID	Pyrrole concn. [w/v%]	Silica concn. [w/v%]	Oxidant concn. [w/v%]	PPY content[a] [wt%]	σ[b] [S cm^{-1}]	Weight-average diameter[c] [nm]
18	0.50	0.50	4.55	82.7	3×10^{-3}	870 ± 610
8	1.00	1.00	9.10	61.6	1	250 ± 50
19	2.00	2.00	18.20	57.7	5	390 ± 180
20	3.00	3.00	27.30	53.5	5	380 ± 180
21	4.00	4.00	36.40	57.1	3	390 ± 200

$FeCl_3 \cdot 6H_2O$ was used as the oxidant in all polymerizations, which were carried out in 100 ml water at 25 °C for 24 h using the 20 nm silica sol.
[a] By CHN elemental microanalysis.
[b] By four-point probe method on compressed pellets.
[c] By disc centrifuge photosedimentometry.

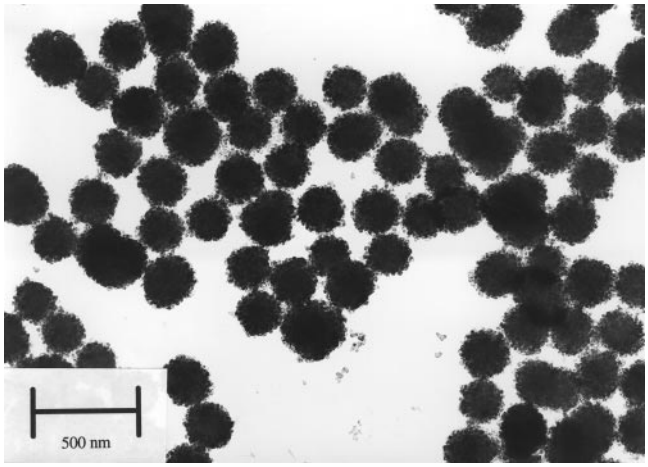

Fig. 2 Typical transmission electron micrograph of polypyrrole–silica nanocomposite particles obtained using the $FeCl_3 \cdot 6H_2O$ oxidant at 20 °C at an initial silica concentration of 1.0 w/v%

Maeda and Armes have previously reported [7] that, prior to addition of the pyrrole monomer, Fe^{3+} ions adsorb onto the surface of the ultrafine silica sol. Thus in the synthesis of polypyrrole–silica nanocomposites the initial locus of polymerization is likely to be at the surface of the silica particles. As the amount of silica in the reaction is increased, the total surface area of silica and the amount of adsorbed Fe^{3+} is also increased, thus the polypyrrole layer formed is less likely to be continuous. This may account for the lower conductivities of entries 15–17. During the first centrifugation–redispersion cycle it was also noted that the reaction supernatants were brown for entries 15–17. This suggests that the excess pyrrole monomer in the reaction led to the formation of soluble pyrrole oligomers in the reaction solution.

Lowering both the pyrrole and the silica concentrations (entry 13) resulted in a nanocomposite with a surprisingly high polypyrrole content (ca. 81%) and slightly larger, more polydisperse particles than those obtained using the "standard" formulation. The reason(s) for these differences remain unclear at present.

Effect of varying pyrrole, oxidant and silica sol concentrations

This series of experiments were carried out using only the $FeCl_3 \cdot 6H_2O$ oxidant, which has relatively high solubility in aqueous media. Reagent concentrations were varied relative to the "standard" formulation for nanocomposite syntheses.

Halving the pyrrole, $FeCl_3 \cdot 6H_2O$ and silica sol concentrations (entry 18 in Table 4) led to the formation of

large nanocomposite particles and an extremely broad PSD, which suggests significant flocculation. Again, it appears that a relatively high polypyrrole content (ca. 83%) does not necessarily lead to high conductivities (cf. entry 13 in Table 3). Simultaneously increasing the pyrrole, oxidant and silica concentrations by a factor of two, three or four (entries 19–21) yields nanocomposites of very similar particle size, polypyrrole content and conductivity. This is surprising given that increasing the reagent concentrations might be expected to lead to much faster polymerization rates [23], which might be expected to affect particle size and perhaps have a deleterious effect on conductivity. All three nanocomposites apparently had a weight-average diameter of just under 400 nm, as judged by DCP. This average size was, however, misleading. These dispersions each have bimodal distributions, with a primary population at 200–250 nm, and a secondary population at around 500 nm (see Fig. 3). The secondary peak may indicate some degree of weak flocculation.

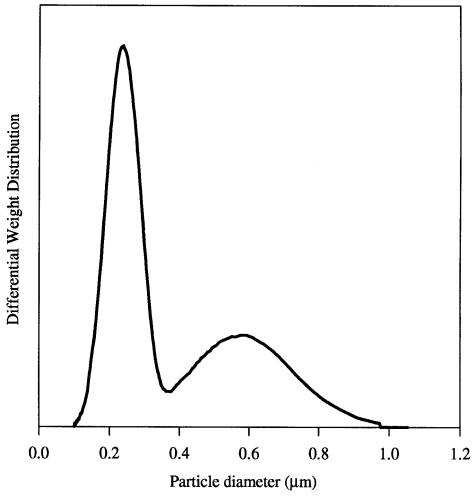

Fig. 3 Bimodal particle size distribution obtained for entry 21 (Table 4) using disc centrifuge photosedimentometry

Effect of silica particle diameter

TEM studies indicated that the 100 nm diameter silica sol was relatively monodisperse whereas the 300 nm diameter silica sol was rather polydisperse, containing a considerable number of particles in the 50–150 nm diameter size range. Thus the manufacturer's nominal diameter for the latter sol should be treated with some caution.

The nanocomposites synthesized using both the 100 and 300 nm diameter silica sols were colloidally unstable, flocculating approximately 1 h after addition of the pyrrole monomer. After clean-up it was possible to redisperse the particles sufficiently in order to obtain a reasonable DCP analysis.

It is clear from Table 5 that increasing the silica sol diameter from 20 up to 300 nm leads to larger polypyrrole–silica nanocomposites, as expected. However, significantly lower polypyrrole contents and conductivities were obtained for nanocomposites prepared using the 50, 100 and 300 nm sols. These conductivities suggest that very little polypyrrole is present at the surface of the nanocomposites, leading to poor electrical contact between adjacent particles at the microscopic level. The maximum theoretical polypyrrole contents for entries 23 and 24 are 18.7 and 7.1 wt%, respectively (assuming that all of the silica sol was incorporated into the composite). Since the polypyrrole contents of these samples are so close to the theoretical values, it is probable that the polypyrrole and silica are merely co-precipitating rather than forming colloidal nanocomposite structures. Similar observations were made by Armes et al. who polymerized pyrrole in the presence of a micrometer-sized silica sol [24]. This hypothesis is supported by the gross flocculation of these dispersions only 1 h after pyrrole addition.

Effect of oxidant

Table 6 summarizes the data obtained from nanocomposites synthesized using three different oxidants. Entries

Table 5 Effect of silica sol diameter on the particle size, conductivity and chemical composition of the resulting polypyrrole–silica nanocomposites

Sample ID	Silica size [nm]	Silica concn. [w/v%]	PPY content[a)] [wt%]	σ[b)] [S cm^{-1}]	Weight average diameter[c)] [nm]
8	20	1.00	61.6	1	250 ± 50
22	50	2.50	32.9	4.3×10^{-3}	240 ± 60
23	100	5.00	18.5	$<10^{-6}$	440 ± 130
24	300	15.00	7.1	$<10^{-6}$	770 ± 180

Reactions were carried out at 25 °C for 24 h using 1.00 ml pyrrole and 9.10 g $FeCl_3 \cdot 6H_2O$ in 100 ml water.
[a)] By CHN elemental microanalysis.
[b)] By four-point probe method on compressed pellets.
[c)] By disc centrifuge photosedimentometry.

Colloid & Polymer Science, Vol. 276, No. 10 (1998)
© Steinkopff Verlag 1998

Table 6 Effect of oxidant type on the particle size, conductivity and chemical composition of the resulting polypyrrole–silica nanocomposites

Sample ID	Oxidant type	Pyrrole concn. [w/v%]	Silica concn. [w/v%]	PPY content[a] [wt%]	σ[b] [S cm^{-1}]	Weight average diameter[c] [nm]
8	$FeCl_3 \cdot 6H_2O$	1.00	1.00	61.6	1	250 ± 50
11	$(NH_4)_2S_2O_8$	1.00	1.00	51.8	6×10^{-3}	180 ± 40
25	H_2O_2/Fe^{3+}/HBr	3.00	5.25	~55.0	7.5×10^{-3}	180 ± 30

Reactions using $FeCl_3 \cdot 6H_2O$ and $(NH_4)_2S_2O_8$ were carried out in deionized water at 25 °C for 24 h using an oxidant : pyrrole molar ratio of 2.33 : 1 and the 20 nm diameter silica sol. For details of the H_2O_2/Fe^{3+}/HBr reaction, see experimental section.
[a] By CHN elemental microanalysis.
[b] By four-point probe method on compressed pellets.
[c] By disc centrifuge photosedimentometry.

8 and 11 are taken from Tables 2 and 4, respectively; they are presented again to aid comparison with entry 25. Use of the H_2O_2/Fe^{3+}/HBr catalytic oxidant as described by Yamamoto and co-workers [25] resulted in nanocomposite particles which are very similar in character to those synthesized using the $(NH_4)_2S_2O_8$ oxidant. In an attempt to improve the conductivity of the particles synthesized using the H_2O_2/Fe^{3+} oxidant, *p*-toluenesulfonic acid was used instead of HBr as the added acid. Thus the tosylate ion was expected to replace the bromide ion as the major dopant anion for the cationic polypyrrole chains. Such aromatic sulfonate dopants are known to improve the conductivity of polypyrrole [26]. However, the resulting nanocomposite has only a marginally higher conductivity (ca. 10^{-2} S cm^{-1}) and the particles were colloidally unstable as judged by DCP.

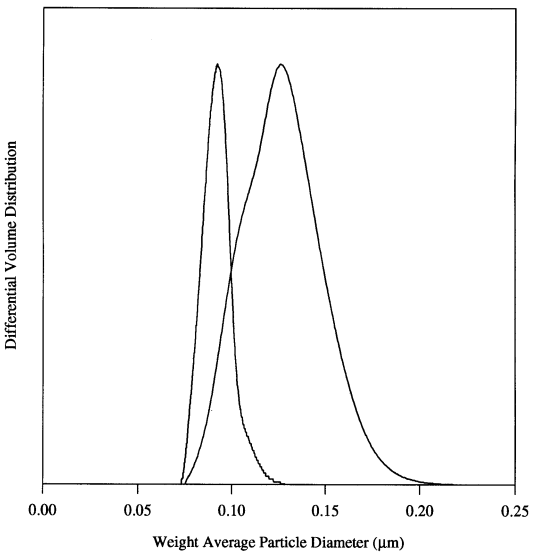

Fig. 4 Effect of stirring rate on the particle size distribution of polypyrrole–silica nanocomposite particles as judged by disc centrifuge photosedimentometry. Synthesis conditions were as follows: $(NH_4)_2S_2O_8$ oxidant at 4 °C at an initial silica concentration of 3.4 w/v%. Note the smaller particle diameter and narrower size distribution obtained using the Silverson stirrer (5000 rpm) compared to magnetic stirring

Effect of stirring rate

As far as we are aware, there has been only one literature report of the effect of stirring rate on the formation of conducting polymer particles. For the synthesis of sterically stabilized polyaniline dispersions using poly(vinyl alcohol) or poly(*N*-vinylpyrrolidone) stabilizers, Stejskal et al. [27] reported that stirring was *detrimental* to colloid formation. The dramatic effect of a faster stirring rate is illustrated in Fig. 4. With conventional magnetic stirring a relatively broad particle size distribution was obtained using the $(NH_4)_2S_2O_8$ oxidant, with a weight-average particle diameter of 134 ± 25 nm (NB a rather higher silica sol concentration of 3.4 w/v% was used in this experiment, which led to a slightly smaller particle size than that indicated by entry 12 in Table 2). However, using the Silverson stirrer under the same conditions resulted in a much narrower particle size distribution, with a significantly reduced weight-average particle diameter of 92 ± 10 nm. On the other hand, the polypyrrole contents of these two dispersions were fairly similar at 38% (magnetic stirring) and 42% (Silverson stirring at 5000 rpm), respectively. This stirring rate effect on particle size was completely reproducible: very similar results were obtained from three separate Silverson syntheses. Surprisingly, the effect of higher stirring rates on the $FeCl_3$-synthesized polypyrrole–silica particles was much less apparent. It is well known [22] that the $(NH_4)_2S_2O_8$ oxidant polymerizes pyrrole much faster than $FeCl_3$. Thus it is perhaps understandable that the much more rapid and efficient mixing of reagents achieved with the Silverson stirrer has a bigger influence on the size distributions of polypyrrole–silica particles synthesized using the former oxidant. It is noteworthy that smaller, more monodisperse

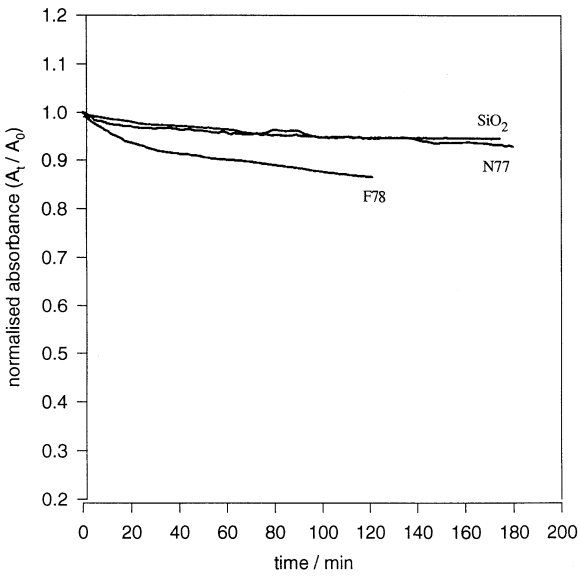

Fig. 5 Absorbance vs. time curves obtained for (a) silica, (b) a $FeCl_3$-synthesized polypyrrole–silica nanocomposite (entry 8 in Table 6) and (c) a $(NH_4)_2S_2O_8$-synthesized polypyrrole–silica nanocomposite (entry 11 in Table 6) in the presence of 0.10 M KCl at 25 °C. The colloid stability of the $(NH_4)_2S_2O_8$-synthesized polypyrrole–silica nanocomposite is very similar to that of the silica sol and is superior to that of the $FeCl_3$-synthesized polypyrrole–silica nanocomposite

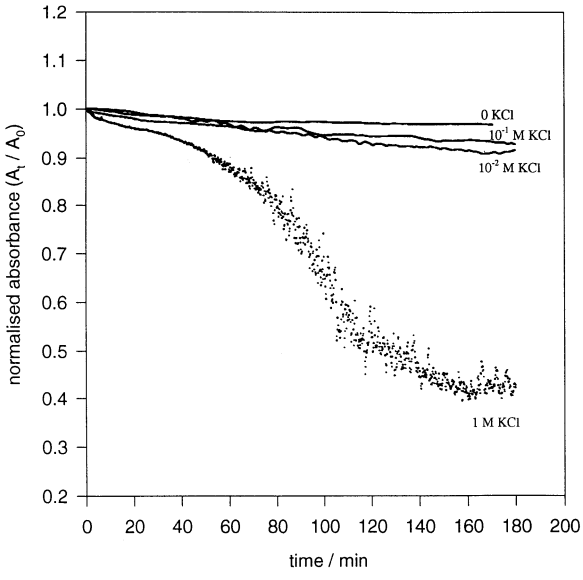

Fig. 6 Absorbance vs. time curves obtained for a $(NH_4)_2S_2O_8$-synthesized polypyrrole–silica nanocomposite (entry 11 in Table 6) in the presence of 0.00, 0.01, 0.10 and 1.00 M KCl at 25 °C. Note the very poor colloid stability (rapid decrease in absorbance) obtained at the highest salt concentration

polypyrrole–silica particles may perform better as "marker" particles in immunodiagnostic strip assays since they will diffuse faster and more uniformly than larger, more polydisperse particles [28].

Colloid stability

The absorbance vs. time plots shown in Fig. 5 indicate that the colloid stability of $(NH_4)_2S_2O_8$-synthesized polypyrrole–silica particles in 0.10 M KCl at 25 °C is comparable to that of a similar-sized silica sol, whereas the $FeCl_3$-synthesized polypyrrole–silica particles are markedly less stable under the same conditions. These results are in good agreement with the X-ray photoelectron spectroscopy studies reported by Maeda et al. [11], who showed that the surface compositions of $(NH_4)_2S_2O_8$-synthesized polypyrrole–silica particles were distinctly more silica-rich than polypyrrole–silica particles prepared using $FeCl_3$. In addition, Butterworth et al. [10] recently reported that the zeta potential vs. pH curves of a series of polypyrrole–silica dispersions were superimposable on that obtained for conventional silica particles. The effect of increasing electrolyte concentration on the colloid stability of the $(NH_4)_2S_2O_8$-synthesized polypyrrole–silica dispersion is shown in Fig. 6. As expected, the highest colloid stability was observed in the absence of KCl and the dispersion became flocculated in 1.0 M KCl. Reasonable (and very similar) colloid stabilities were obtained at the two intermediate KCl concentrations (0.01 and 0.10 M). Bearing in mind the peculiarly high resistance to salt-induced flocculation exhibited by conventional silica sols [29], these colloid stability results are consistent with a charge stabilization mechanism for these nanocomposite particles.

Conclusions

The particle size and chemical composition of polypyrrole–silica nanocomposites prepared using $FeCl_3 \cdot 6H_2O$ are remarkably insensitive to a wide range of synthesis parameters, including oxidant, monomer and silica sol concentrations, silica sol diameter and polymerization temperature. This is rather surprising since Maeda and Armes had previously demonstrated that varying two other parameters, the silica sol concentration and the nature of the oxidant, had a considerable effect on the particle size and the silica content of the nanocomposites.

One synthesis parameter which does have a significant and reproducible effect is the stirring rate. Smaller, more monodisperse nanocomposite particles are obtained from rapidly stirred reaction solutions. However, this effect is only observed when using the $(NH_4)_2S_2O_8$ oxidant. An alternative oxidant, H_2O_2/Fe^{3+}, was found to give

© Steinkopff Verlag 1998

nanocomposites of similar particle size, polypyrrole content and conductivity to those obtained using the $(NH_4)_2S_2O_8$ oxidant.

The colloid stability of these polypyrrole–silica nanocomposite particles depends on their silica content. The colloid stability of a silica-rich nanocomposite prepared using the $(NH_4)_2S_2O_8$ oxidant was comparable to that of a silica sol of similar size in the presence of electrolyte, whereas a polypyrrole-rich nanocomposite prepared using $FeCl_3$ had markedly poorer colloid stability under these conditions. These observations are consistent with earlier XPS studies, which indicated that the surface compositions of $(NH_4)_2S_2O_8$-synthesized nanocomposites are much more silica-rich (as judged by their Si/N atomic ratios) than $FeCl_3$-synthesized nanocomposites. Thus the combined experimental evidence suggests a charge stabilization mechanism for these nanocomposite particles.

Acknowledgements The Defence Research Agency is thanked for funding a PhD studentship for SFL. MDB and GPM wish to thank the EPSRC for funding their post-doctoral studies at Sussex (GR/H93606 and GR/K01841 awards, respectively). SPA also wishes to acknowledge the EPSRC for funding the purchase of the disc centrifuge photosedimentometer.

References

1. Bradner FP, Shapiro JS, Bowley HJ, Gerrard DL, Maddams WF (1989) Polymer 30:914–917
2. Bjorklund RB, Liedberg B (1986) J Chem Soc Chem Commun 1293–1295
3. Armes SP, Vincent B (1987) J Chem Soc Chem Commun 288–290
4. Cawdery N, Obey TM, Vincent B (1988) J Chem Soc Chem Commun 1189–1190
5. Simmons MR, Chaloner PA, Armes SP (1995) Langmuir 11:4222–4224
6. Maeda S, Armes SP (1993) J Colloid Interface Sci 159:257–259
7. Maeda S, Armes SP (1994) J Mater Chem 4:935–942
8. Maeda S, Armes SP (1995) Synth Met 69(1–3):499–500
9. Maeda S, Armes SP (1995) Chem Mater 7:171–178
10. Butterworth MD, Maeda S, Johal J, Corradi R, Lascelles SF, Armes SP (1995) J Colloid Interface Sci 174: 510–517
11. Maeda S, Gill M, Armes SP, Fletcher IW (1995) Langmuir 11:1899–1904
12. Maeda S, Armes SP (1995) Synth Met 73(2):151–155
13. Gill M, Mykytiuk J, Armes SP, Edwards JL, Yeates T, Moreland PJ, Mollett C (1992) Chem Commun 108
14. Stejskal J, Kratochvil P, Lascelles SF, Armes SP, Riede A, Helmstedt M, Prokes J, Krivka I (1996) Macromolecules 29:6814–6819
15. Corradi R, Armes SP, unpublished results
16. Terrill NJ, Crowley T, Gill M, Armes SP (1993) Langmuir 9:2093–2096
17. Maeda S, Armes SP (1994) ACS Polym Prep 35(1):217–218
18. Pope MR, Tarcha PJ, Armes SP (1996) Bioconjugate Chem 7:436–444
19. Maeda S, Corradi R, Armes SP (1995) Macromolecules 28(8):2905–2911
20. McCarthy GP, Armes SP, Greaves SJ, Watts JF (1997) Langmuir 13:3686–3692
21. Iler RK, McQueston HJ (1974) US patent No 3,855,172
22. Riede A, Helmstadt M, Riede V, Stejskal J (1997) Colloid Polym Sci 275(9): 814–820
23. Bjorklund RB (1987) J Chem Soc Faraday Trans I 83:1507–1514
24. Armes SP, Gottesfeld S, Beery JG, Garzon F, Agnew SF (1991) Polymer 32(13): 2325–2330
25. Liu CF, Moon D-K, Maruyama T, Yamamoto T (1993) Polym J 25:775–779
26. Armes SP, Aldissi M (1990) Polymer 31:569–574
27. Stejskal J, Kratochvil P, Helmstadt M (1996) Langmuir 12(14):3389–3392
28. Kawaguchi H (1993) In: Tsuruta T, Hayashi T, Kataoka K, Ishihara K, Kimura Y (eds) Biomedical Applications of Polymeric Materials. CRC Press, London, 299–324
29. Healey TW, Berga HE, (eds) ACS Symp Ser No. 234, American Chemical Society, Washington DC, USA, 147–159